SLAC–PUB–6582
August, 1994
(T/E)

Complementarity of e^+e^- and pp Colliders for the Exploration of Electroweak Symmetry Breaking

MICHAEL E. PESKIN*

Stanford Linear Accelerator Center
Stanford University, Stanford, California 94309

Invited lecture presented at the
22nd INS Symposium on Physics with High Energy Colliders
University of Tokyo
March 8–10, 1994

⋆ Work supported by the Department of Energy, contract DE–AC03–76SF00515.

Complementarity of e^+e^- and pp Colliders for the Exploration of Electroweak Symmetry Breaking

Michael E. PESKIN

Stanford Linear Accelerator Center
Stanford University, Stanford, California 94309

Abstract: I review the physics capabilities of the machines proposed for the next generation of high-energy experimentation: in hadron physics, the LHC, and in electron physics, a 500–1500 GeV e^+e^- linear collider. Using for illustration two specific models of electroweak symmetry breaking, I show how the pp and e^+e^- techniques are expected to complement one another in the exploration of the next scale of physics.

1. Introduction

When we look forward to the future of elementary particle physics, we anticipate discoveries of new particles and phenomena at increasingly higher energies. To plan for this future, we need to design and construct accelerators which access these new energy regimes. It is well appreciated, though, that this planning raises many difficulties. New facilities for high-energy physics are extremely complex, requiring a decade or more for their planning and construction. They are also extremely expensive, so much so that the high energy accelerators of the future will require funding through international collaboration. Thus, we must evolve a persuasive plan that is scientifically grounded and can win wide acceptance.

Our situation would be made easier if there were a single ideal machine design which would allow us to answer our most pressing questions. Over the history of our field, there have been many claims that a particular machine configuration would provide the essential clues that we are seeking. In the United States, both the SLAC and Fermilab accelerators were proposed by men with intense, and completely divergent, personal visions of the correct next step in high-energy physics. More recently, we have seen the SSC put forward in the United States as the crucial accelerator for the future, only to leave a vacuum in our national planning when the SSC project was cancelled last year. Still, historically, however powerful the claims and even the achievements of a particular technique have been, our understanding of physics has grown through the synthesis of experimental information from many sources. Thus, as we evolve our global plan, this should include different types of experimental facilities which complement one another.

The most technically promising means to achieve the next step in center of mass energy are through proton-proton and electron-positron colliders. On the proton-proton side, the next step is almost assured through the fact that CERN has made the Large Hadron Collider (LHC) its highest priority project [1]. This project should give us access to parton-parton collisions at multi-TeV energies. On the electron-positron side, the situation is more uncertain. The technical feasibility of the next collider is now clear, with prototypes of all of the major components now completed or under construction at laboratories around the world. There are now several competing designs for machines that would begin operation at 400-500 GeV and would be expandable in energy up to about 1.5 TeV [2,3]. However, it is much less clear, at least to the broader world community, what role the next e^+e^- collider would play in relation to the high-energy experiments being done on the proton-proton side.

It is this question that I would like to address: How will experiments at the next e^+e^- collider complement experiments to be done at the next pp collider, and what e^+e^- center-of-mass energy is needed to achieve the best match between these facilities?

In discussions among physicists, and even in the literature, one often sees facile and oversimplified answers to these questions. It is argued, for example, that pp and e^+e^- facilities are complementary only when they have comparable parton center-of-mass energy, or that proton machines are best for 'discovery' while e^+e^- facilities are best for 'precision studies'. The history of the discovery of ingredients of the standard model of course gives a more complicated picture. For example, the gluon was discovered at an e^+e^- collider, while quantitative information on its interactions was derived from $p\overline{p}$ experiments. Thus, we must check our preconceptions against detailed analysis. A purely historical approach, however, may not extrapolate simply to the problems of future experimentation.

In this lecture, I will take a different approach which concentrates on a general issue of great importance to the future colliders. Elementary particle physicists have now established the standard model gauge theory of strong, weak, and electromagnetic interactions. This theory has met stringent quantitative tests, particularly in the sector of high-energy weak interactions. But the theory has an obvious difficulty: It requires that the weak interaction gauge symmetry $SU(2) \times U(1)$ be spontaneously broken, but it does not provide a physical mechanism for this symmetry breaking. One cannot approach most of the remaining mysteries of particle physics—in particular, the questions of the nature and mass spectrum of the quarks and leptons—without understanding the solution to this problem. Since the mass scale of electroweak symmetry breaking is the W mass scale, the solution to this problem should soon be experimentally accessible. This problem was given as the main justification for building the SSC, and it must figure strongly in the motivation for any other future collider. Indeed, because of the successes of the standard electroweak model in its confrontation with experiment, the impetus to solve this problem is even greater now than it was ten years ago.

Models of many different types have been proposed to solve the problem of electroweak symmetry breaking. Every such model entails new particles and forces. At this moment, we have very little information to discriminate these models. But in the era of the next generation colliders, we should expect to discover these new particles and begin the exploration of a new sector of the fundamental interactions.

To analyze the requirements for this exploration, I will review the properties of two representative models of electroweak symmetry breaking and the experiments at future pp and e^+e^- colliders that should give us experimental insights into their structure. Realistic models of electroweak symmetry breaking are complex and multifaceted. By analyzing the variety of phenomena associated with a given model, we will gain an appreciation of the richness of the phenomena which should be uncovered at the next scale. At the same time, we will obtain a concrete picture of the complementary roles that pp and e^+e^- experiments would play in the experimental elucidation of each model. At the end of the lecture, I will contrast the results of these explicit analyses with the standard rules of thumb on the comparison of colliders.

2. Two Models of Electroweak Symmetry Breaking

Since the main thrust of this lecture will involve the analysis of theoretical models, I should begin by justifying my choice of models to examine. In the literature, one finds many models of electroweak symmetry breaking with one or more Higgs doublet fields, more complex particle multiplets, and possibly complicated strong-coupling dynamics. Which should we take as our examples?

The minimal model of electroweak symmetry breaking contains a single Higgs field and gives rise to only one new particle, the minimal Higgs boson. Many authors have taken it as the basis for detailed studies. However, in my opinion, this model cannot be taken seriously as a fundamental theory. The model has well-known pathologies: These include the gauge hierarchy problem, the fact that the natural value of the W mass in this model is the grand unification or Planck scale [4]. In addition, in this model, all parameters of the quark and lepton mass matrices are renormalizable coupling constants which must be input to define the theory and which thus cannot be predicted. These pathologies are an inevitable part of the minimal package; they characterize the fact that the minimal Higgs model does not explain electroweak symmetry breaking but, rather, is simply a parametrization of this phenomenon. In order to explain electroweak symmetry breaking, we need to consider models which contain richer dynamical possibilities.

Models that present a mechanism for $SU(2) \times U(1)$ breaking fall into one of two classes, depending on whether the Higgs boson is taken to be elementary or composite. If the model includes an elementary Higgs field, it must contain some mechanism to cancel the arbitrary additive mass renormalization of this scalar field. The only known mechanism to achieve this cancellation is supersymmetry. The assumption of supersymmetry brings in a new sector of particles and a complex array of new interactions. However, it also brings some important advantages: Within supersymmetry, there is a natural mechanism for $SU(2) \times U(1)$ breaking, since the Higgs field which couples to the heavy top quark obtains a negative $(\text{mass})^2$ renormalization. The supersymmetric renormalization group equations also naturally relate the values of the coupling constants obtained at LEP to the predictions of a grand unified gauge theory. These and other features of supersymmetric models are reviewed in Refs. [5–7].

If the model does not include an elementary Higgs field, some new strong interaction dynamics must be provided to create the composite state which acquires a vacuum expectation value. The simplest way to achieve this is by postulating a new strong interaction gauge theory of fermions at a mass scale of about 1 TeV. Then the breaking of $SU(2) \times U(1)$ can proceed by the same mechanism that breaks chiral $SU(2) \times SU(2)$ in the familiar strong interactions. In a theory constructed in this way, the new strong interaction is called technicolor. General aspects of technicolor models are reviewed in Refs. [8–9].

In principle, there are many other ways in which new interactions at the 1 TeV mass scale can induce the breakdown of $SU(2) \times U(1)$. However, the two examples of supersymmetry and technicolor models have a particular advantage for the type of study that I will describe here. Since supersymmetry models involve only weak-coupling dynamics, all relevant masses and cross sections can be computed from the underlying parameters of the theory. In technicolor models, one does not have quite so much predictive power, but the properties of the new strong interactions can be computed using phenomenological methods borrowed from the study of the familiar strong interactions. Thus, for both types of model, there is a sizable literature on the signatures of the new sector at future colliders. We can make use of this literature to understand in detail the relation of e^+e^- and pp experiments.

I repeat that, in this lecture, I am not arguing that one of these models must be correct. It is quite likely that that solution of the problem of electroweak symmetry breaking is more subtle, and that it will require experimental elucidation. What I am arguing is that we should take known solutions to this problem seriously as illustrative possibilities for the next scale in physics, and that we should pay attention to the lessons they have to teach us.

Both supersymmetry and technicolor models are complex, and both provide a wide variety of particles and phenomena that the new colliders should make visible. It is not true in either model that a single discovery (for example, the sighting of a Higgs boson) would clarify the physics. Rather, this discovery would be only the first step in a long and fascinating investigation. In the models we have anticipated, we can work out in detail what tools we will need for this investigation. If Nature has chosen a model that we have not anticipated, we presumably will need even more experimental guidance. And even if these tools will be needed only ten years from now, we must immediately set in motion the technical and political processes that will make them available.

3. 'Discovery Reach'

The simplest criterion for comparing the capabilities of e^+e^- and pp machines is the parton-parton center of mass energy available to produce new particles. This criterion is often referred to as the 'energy' or 'discovery reach' of a collider. I will argue later in this lecture that this criterion is naive. Still, it is interesting to know, as a point of reference, what this criterion predicts.

The usual way of making this comparison is to choose a sample list of new physics processes, compare the energy needed to discover each at a variety of colliders, and then form some sort of average. Comparisons of this type can be found, for example, in Refs. [10–13].

If the exotic particles under consideration have electroweak quantum numbers, they can be pair-produced at e^+e^- colliders. Typically, such particles can be produced for masses almost up to $\sqrt{s}/2$ for reasonable samples of integrated luminosity. As a striking example of this sensitivity, one might consider the search limits reported by the Mark II experiment at the SLC in Ref. [14], using a data sample of 500 Z^0 events. In the remainder of this lecture, I will assume that future e^+e^- colliders will produce event samples of about 3000 events per year per unit of R, comparable to the event samples of PEP and PETRA. This requires a luminosity increasing with energy according to

$$\mathcal{L} \sim 10^{33} \frac{E_{\rm CM}^2}{(500 \text{ GeV})^2} \text{ cm}^{-2}\text{sec}^{-1} . \tag{1}$$

This estimate is a factor 4–10 lower than current design luminosities for the next generation linear collider.

The discovery reach of a pp collider is more difficult to estimate. For any given new particle, one must find a signature which can be observed in the pp environment, define cuts which isolate this signature from background, and then compute the number of pp collisions required to produce a significant number of signal events passing the cuts. A comprehensive study of this kind was assembled ten years ago by Eichten, Hinchliffe, Lane, and Quigg in their review of supercollider physics [11]. In the intervening time, many of the analyses they presented have been made more sophisticated by inclusion of the effects of hadronization and realistic detectors, but the results of their paper can still be used as a benchmark for broad comparisons.

In Fig. 1, I show a comparison of the discovery limits estimated in Ref. [11] with those appropriate to e^+e^- colliders for five particular new physics effects—a new W boson, a heavy quark, a gluino, a heavy lepton, and a nonzero scale of quark and lepton compositeness [12]. The comparable e^+e^- and pp center of mass energies are given for a fixed pp luminosity of $10^{33}\text{cm}^{-2}\text{sec}^{-1}$ and an e^+e^- luminosity scaling according to (1). One can make similar figures for different assumptions about the pp luminosity.

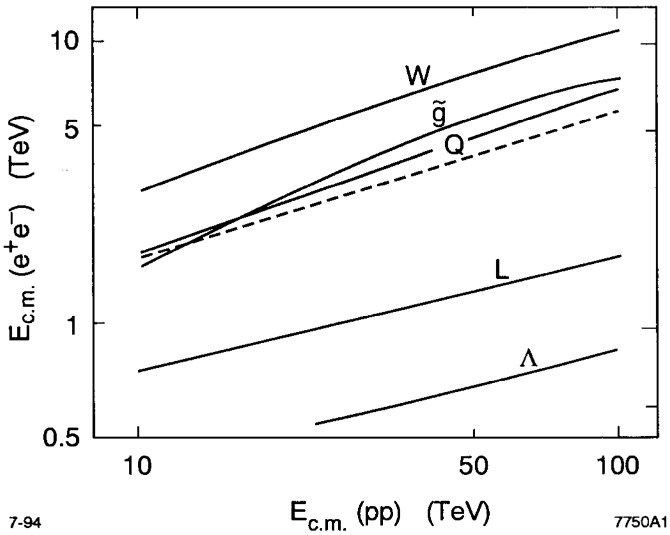

Figure 1. Comparison of the capabilities of e^+e^- and pp colliders to discover five representative signatures of new physics, from Ref. [12], assuming a pp luminosity of $10^{33}\mathrm{cm}^{-2}\mathrm{sec}^{-1}$. The various signatures are: a new W boson, a heavy quark, a gluino, a heavy lepton, and a nonzero compositeness scale Λ. For pp colliders, the discovery reach was taken from Ref. [11]. For e^+e^- colliders, the discovery $\sqrt{s}$ values were taken to be m_W, $2m_Q$, $3m_{\tilde{g}}$, $2m_L$, $\Lambda/30$, respectively, for the five signatures. The first of these estimates assumes that there is also a new Z; the last reflects the experience of PEP and PETRA.

An average comparison is indicated in Fig. 1 as the dashed line. This average corresponds to

$$E_{e^+e^-} \simeq 0.6\big[E_{pp}\big]^{1/2}\big[\mathcal{L}_{pp}\big]^{1/6} , \tag{2}$$

where energies are in TeV and the proton-proton luminosity is in units of 10^{33}. The dependence on luminosity realizes Kane's rule of thumb [10]: a factor 2 in energy is worth a factor 10 in luminosity. Putting in the parameters of the LHC (including extrapolation to 10^{34} luminosity), one finds an equivalent e^+e^- center of mass energy of about 3 TeV.

There are many reasons, however, why this comparison does not tell the full story. I have already noted that this sort of comparison concentrates excessively on the first signal of new physics, and that it depends on arbitrary assumptions about this signature. But, more importantly, this comparison ignores the fact that e^+e^- and pp colliders would typically observe different facets of a new sector of interactions. In the models reviewed in the previous section, the physics which leads to electroweak symmetry breaking is complex and leads to new phenomena both in electroweak and in strong interaction physics. To understand the interrelation between the observables for e^+e^- and pp colliders, one must investigate the models in more detail. In the next several sections, I will review the predictions of supersymmetry and technicolor models from this point of view. We will see that these two complete disparate approaches to the problem of electroweak symmetry breaking lead to similar conclusions about the comparison of colliders, conclusions which are in both cases very different from the simple scaling law of Eq. (2).

4. Supersymmetry: Higgs Sector

In this section and the next, I will compare the signatures of the minimal supersymmetric standard model for e^+e^- and pp colliders. Supersymmetry is an example of a theory of electroweak symmetry breaking in which all of the dynamics occurs as the result of weak-coupling physics. For this reason, the consequences of the model are computable in great detail, and a wide variety of signatures have been studied quantitatively.

If indeed Nature has chosen supersymmetry as the explanation for electroweak symmetry breaking, the most important experimental issues for the next generation of colliders will be the discovery of the new particles present in this model, including the multiplet of Higgs bosons, and the measurement of their couplings. The most important questions for e^+e^- and pp colliders are summarized in Table 1. These questions divide into two parts. First, supersymmetry necessarily includes an extended Higgs boson sector which could, in principle, be found in more general weakly-coupled models. In this section, I will discuss the study of this sector at future colliders. Second, supersymmetry predicts a characteristic doubling of the spectrum of elementary particles, with scalar partners of the quarks and lepton and fermionic partners of the gauge bosons. I will discuss the study of these particles in the following section.

In supersymmetric models, the same Higgs field cannot give mass to both the d and u type quarks through Yukawa couplings invariant under supersymmetry [5]. Thus, supersymmetric models require two Higgs doublet fields ϕ_1, ϕ_2. After the components eaten by $W^\pm$ and Z^0 are removed, this sector contains three neutral bosons plus the charged pair $H^\pm$. The neutral bosons are derived from the underlying fields by rotation through the mixing angles α and β:

$$\begin{aligned} CP \text{ even}: &\quad \begin{pmatrix} \mathrm{Re}\,\phi_1 \\ \mathrm{Re}\,\phi_2 \end{pmatrix} \xrightarrow{\alpha} \begin{pmatrix} h^0 \\ H^0 \end{pmatrix} \\ CP \text{ odd}: &\quad \begin{pmatrix} \mathrm{Im}\,\phi_1 \\ \mathrm{Im}\,\phi_2 \end{pmatrix} \xrightarrow{\beta} \begin{pmatrix} \pi^0 \\ A^0 \end{pmatrix} . \end{aligned} \tag{3}$$

The field π^0 is eaten by the Z^0; the remaining three fields on the right are associated with physical particles. The mixing angle β is related to the ratio of vacuum expectation values,

$$\tan\beta = \frac{\langle\phi_2\rangle}{\langle\phi_1\rangle}\ ; \tag{4}$$

this angle enters as a parameter throughout supersymmetry phenomenology. In particular, when $\tan\beta$ is large, the b quark and τ lepton typically have large Yukawa couplings to the Higgs sector to compensate the small vacuum expectation value which gives these fermions mass.

Table 1: Supersymmetry

Issues	e^+e^-	pp (LHC)
Higgs:	$m(h^0) < 150\ GeV$	
h^0	visible in $e^+e^- \to Z^0 h^0$ BR measurements for $b\bar{b}, \tau^+\tau^-$, $c\bar{c}, WW^*$, $\Gamma(h^0 \to \gamma\gamma)$	visible in $h^0 \to \gamma\gamma$ in most of parameter space $BR(h^0 \to \gamma\gamma)\Gamma(h^0 \to gg)$
H^0, A^0	visible in $e^+e^- \to H^0 A^0$ up to threshold	visible in $H^0, A^0 \to \tau^+\tau^-$ if $\tan\beta \gtrsim 10$
H^+	visible in $e^+e^- \to H^+H^-$ up to threshold	visible in $t \to bH^+$ if $m_H \lesssim 120\ GeV$
Superpartners: gauginos	$m(\widetilde{\chi}^+) < \frac{1}{4} m(\widetilde{g})$	
	$\widetilde{\chi}^- \widetilde{\chi}^+$ observable up to threshold $\Delta m_\chi / m_\chi \sim 2\%$ for $\widetilde{\chi}^+, \widetilde{\chi}^0$, $m_0, m_{1/2}, \mu \to$ tests of unification, $\widetilde{\chi}_1^+, \widetilde{\chi}_2^+ \to$ tests of supersymmetry	$\widetilde{g}$ observable up to 1.6 TeV in $\not{E}_T$, $\ell^\pm\ell^\pm, \ell Z^0$, $\Delta m\widetilde{g}/m\widetilde{g} \sim 10\%$ under model-dependent hypotheses, $\widetilde{\chi}^+$ observable up to 150 GeV in multileptons
squarks, sleptons	visible in $e^+e^- \to \widetilde{\ell}^+\widetilde{\ell}^-$ up to threshold $\mathcal{O}(1)$ polariz. effects, $\Delta m_\ell / m_\ell \sim 1\%$	visible in $gg \to \widetilde{q}\widetilde{q}$ unless buried by the $\widetilde{g}\widetilde{g}$ signal

In the most general Higgs theories, the mass spectrum of Higgs bosons obeys only a few general constraints. However, the minimal supersymmetric standard model provides some more specific relations among the masses of the Higgs particles. Consider first the lightest Higgs boson h^0. At the tree level, the mass of this particle obeys

$$m(h^0) \leq m_Z \left|\cos 2\beta\right| . \tag{5}$$

This bound is known to be raised by large radiative corrections, but still the upper limit is less than about 130 GeV [15]. In supersymmetric models with more complicated Higgs sectors, there is no such simple formula. Nevertheless, the h^0 mass is still strongly restricted if the theory has a grand unification: Under this assumption, the mass of the lightest Higgs boson is controlled by a coupling constant which must be finite at the grand unification scale and then is run by the renormalization group to smaller values at lower mass scales [16]. One then finds an upper limit of 200 GeV on the mass of the lightest Higgs boson in the broad class of grand unified models. In nonminimal supersymmetric models, the lightest Higgs boson must lie below 150 GeV [17].

For the heavier Higgs bosons, there are no similar upper bounds. However, the masses of these bosons are linked together, in minimal supersymmetry, by relations which read, at the tree level,

$$\begin{aligned} m^2(H^+) &= m^2(A^0) + m_W^2 \\ m^2(H^0) &= m^2(A^0) + m_Z^2 - m^2(h^0) \ . \end{aligned} \tag{6}$$

It is convenient to consider the mass of the A^0 (henceforth, m_A) as setting the scale of these heavier masses. In models of electroweak symmetry breaking through supersymmetry, m_A is typically in the range 200–500 GeV. More details on the supersymmetric Higgs boson spectrum can be found in Refs. [18] and [15].

Each Higgs boson can decay to a pair of fermions or bosons of any lighter species, with branching ratios roughly scaling as the square of the mass of the decay product. Branching ratios to pairs of supersymmetric particles may be larger if these decays are kinematically allowed; in the following discussion, I ignore this possibility. In addition, a Higgs boson can decay to photon or gluon pairs through a one-loop amplitude. These various decay channels offer many possible signatures that can be observed at a hadron collider.

Several groups have studied the visibility of the variety of Higgs boson signatures at the LHC [19–22]. The dominant decay to $b\bar{b}$ is expected to be swamped by hadronic production of $b\bar{b}$ pairs. The most characteristic signature of a light Higgs boson is expected to be the two-photon decay $h^0 \to \gamma\gamma$. This decay is rare and requires high luminosity for its observation, but it is considered a reasonable target for the LHC experiments. The decay to τ pairs can be observed from the sample of 1-prong jets, but the signal is not expected to be sufficient unless the Higgs coupling to $\tau^+\tau^-$ is enhanced; this occurs for H^0 and A^0 decays to τ pairs if the parameter $\tan\beta$ is large. Finally, if the H^0 mass is not too large, this particle can be observed through its decay to Z^0Z^{0*}, that is, one on-shell and one off-shell Z^0. In the minimal supersymmetric standard model, the H^0 decouples from Z^0Z^0 if it is as massive as $2m_Z$. The global picture of the observability of Higgs decays modes in the minimal supersymmetric standard model, as a function of the parameters m_A and $\tan\beta$, is shown in Fig. 2.

Several features of this diagram are worth particular attention. When this diagram was first presented, it was considered remarkable that, in most of the plane, there would be some Higgs signal in this extended Higgs model. On the other hand, for most choices of parameters, there is only a single visible Higgs signature, and not necessarily one that would distinguish this case from the minimal Higgs model. One would directly observe the heavier Higgs boson H^0 and A^0 only in certain regions of parameter space; in fact, one is sensitive to large masses only where the $\tau^+\tau^-$ mode is available at large $\tan\beta$. The only known strategy for observing the H^+ looks for this particle as a decay product of the top

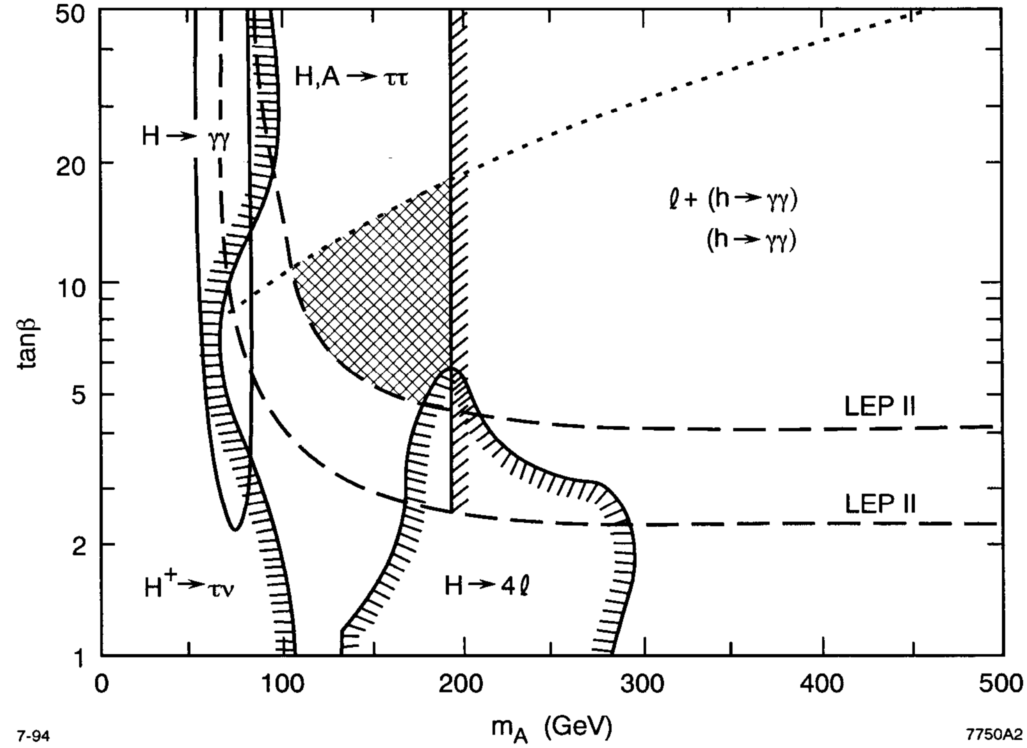

Figure 2. Regions of parameter space in which various signatures of the supersymmetric Higgs sector can be discovered at the LHC, from Ref. [19].

quark and thus is insensitive to charged Higgs particles with mass above about 120 GeV unless $\tan\beta$ is very large [23].

Recently, it has been suggested that Higgs decays to $b\bar{b}$ and $\tau^+\tau^-$ might be made visible at hadron colliders by the use of multiple vertex tags [24,25]. It remains to be seen whether this strategy is can be used effectively at high pp luminosity.

For m_A above 200 GeV, the most important signature is the decay of the light Higgs boson h^0 to two photons. In principle, the rate for producing this signature contains information on the nature of the Higgs boson. However, that information is complicated to extract, since this rate is proportional to the combination

$$\Gamma(h^0 \to gg) \cdot \mathrm{BR}(h^0 \to \gamma\gamma) \ . \tag{7}$$

Both processes are controlled by loop diagrams, as shown in Fig. 3. Gunion and Haber have argued that the process $h^0 \to \gamma\gamma$ is particularly interesting as a probe of exotic particles [26]. One might *assume* that the partial width to gg is dominated by a top quark loop with standard couplings in order to extract the $\gamma\gamma$ branching ratio, but it is not clear how to perform an analysis without such unwanted assumptions.

In e^+e^- colliders, the possibilities for observing the Higgs sector of supersymmetry are much more favorable. The most important processes for the production of Higgs bosons

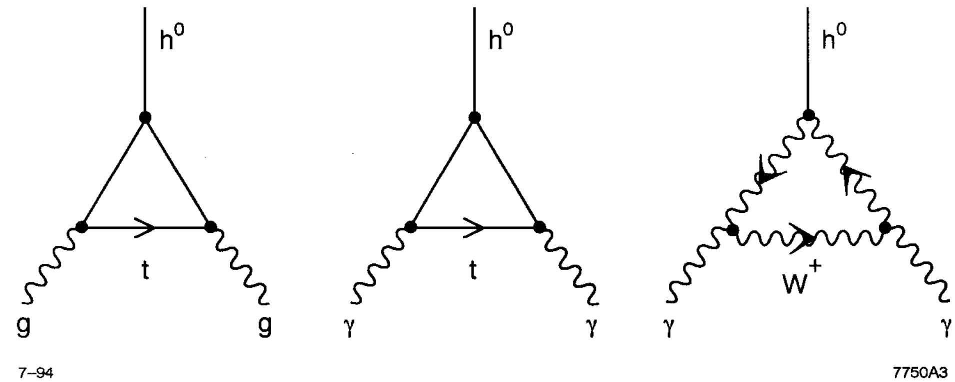

Figure 3. The dominant loop diagrams contributing to the decay processes $h^0 \to gg$ and $h^0 \to \gamma\gamma$, in the minimal standard model. In more complex models, any additional heavy species can also contribute to these amplitudes.

are

$$e^+e^- \to Z^0\mathcal{H}^0 \ , \qquad e^+e^- \to A^0\mathcal{H}^0 \ , \tag{8}$$

where $\mathcal{H}^0$ is h^0 or H^0. These reactions are complementary in a way that Eq. (3) makes clear: A virtual Z^0 links a CP-even state in the top line of (3) to a CP-odd state in the bottom line (where we consider π^0 to be the longitudinal component of a final state Z^0). Whatever linear combination of h^0 and H^0 is produced together with Z^0, the opposite linear combination is produced together with A^0 when the e^+e^- center of mass energy is sufficient. In the minimal supersymmetric standard model, it is h^0 which dominantly couples to Z^0 unless m_A is as small as m_Z.

In the e^+e^- environment, it is expected that Higgs bosons, and also the final state Z^0, can be observed in their hadronic decays modes. For a collider operating at 400 GeV in the center of mass, the process $e^+e^- \to Z^0h^0$ is above threshold for any model arising from grand unification. This process has a substantial rate, of order tenths of a unit of R, and is readily reconstructed [27,28]. A 500 GeV collider would observe all of the particles in the supersymmetric Higgs sector for $m_A < 200$ GeV; for higher values of m_A, one need only increase the center of mass energy proportionally. The analysis which reveals this spectrum can be quite straightforward: Since the Higgs bosons and the Z^0 all have $b\bar{b}$ and $\tau^+\tau^-$ as major decay modes, Janot has suggested looking for $e^+e^- \to (\tau^+\tau^-)(jet\, jet)$ with displaced vertices. A simulation based on this search strategy is shown in Fig. 4 for two choices the of supersymmetry parameters; the mass peaks of h^0, H^0, and A^0 are clearly visible.

Since the h^0 is produced with a readily identified Z^0, it should be straightforward to measure the branching fractions to its major decay modes. Hildreth, Barklow, and Burke have recently analyzed this question with simulation studies, assuming a vertex detector with the capabilities of the one currently operating in the SLD detector [29]. These authors have presented strategies to isolate the $b\bar{b}$, $\tau^+\tau^-$, and WW^* decay modes. A vertex detector closer to the interaction point could also separate the gg and $c\bar{c}$ modes,

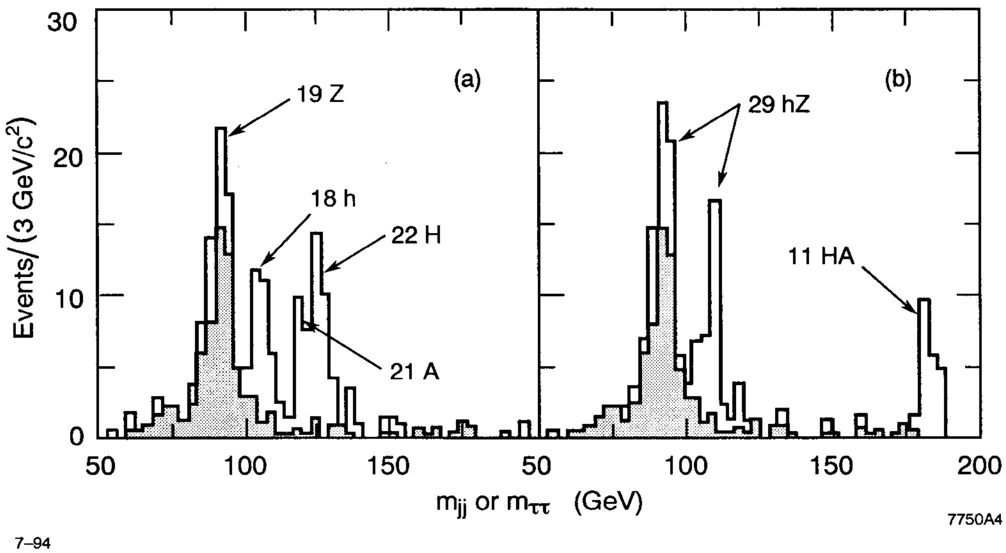

Figure 4. Reconstructed masses of Higgs and Z^0 bosons from the processes (8). These simulations, from Ref. [28], assume 10 fb^{-1} of data at $\sqrt{s} = 400$ GeV, with reconstruction efficiencies modeled by a LEP scale detector. The shaded region is the background, which comes dominantly from $e^+e^- \to Z^0Z^0$. The two figures correspond to (a) $m_A = 120$ GeV, (b) $m_A = 180$ GeV.

which are predicted to have roughly comparable rates. Janot has proposed a set of cuts to measure also the branching ratio into invisible final states, for example, the decay to a pair of neutral supersymmetric particles [28]. The WW^* mode (one real and one virtual W) is particularly interesting because of the relation between the Higgs production and decay vertices,

$$\frac{\mathcal{M}(h^0 \to W^+W^-)}{\mathcal{M}(h^0 \to Z^0Z^0)} = \cos^2\theta_w \ , \tag{9}$$

which assumes only $SU(2) \times U(1)$. Thus, from the WW^* branching ratio and the total h^0 production cross section, one can compute the h^0 total width. The simulation results of Ref. [29] for the measurement of various branching fractions are shown in Fig. 5 for a data sample of 50 fb^{-1}; branching ratio determinations at $m(h^0) = 120$ and 140 GeV are plotted against the theoretical dependence on the h^0 mass and $\tan\beta$. I should note that, in the specific circumstance of the minimal supersymmetry standard model, the model-dependence of branching ratios is not as pronounced as that shown in the bottom figure; the relative size of the $b\bar{b}$ and WW^* branching ratios is proportional to

$$\frac{\sin^2\alpha}{\cos^2\beta\sin^2(\beta-\alpha)} = 1 + 2\cos^2 2\beta \sin^2 2\beta \frac{m_Z^2}{m_A^2} + \cdots \tag{10}$$

in the limit of large m_A.

There is one more possible way to study Higgs bosons at an e^+e^- linear collider: One can backscatter (visible-light) laser beams from the electron beams to create a $\gamma\gamma$

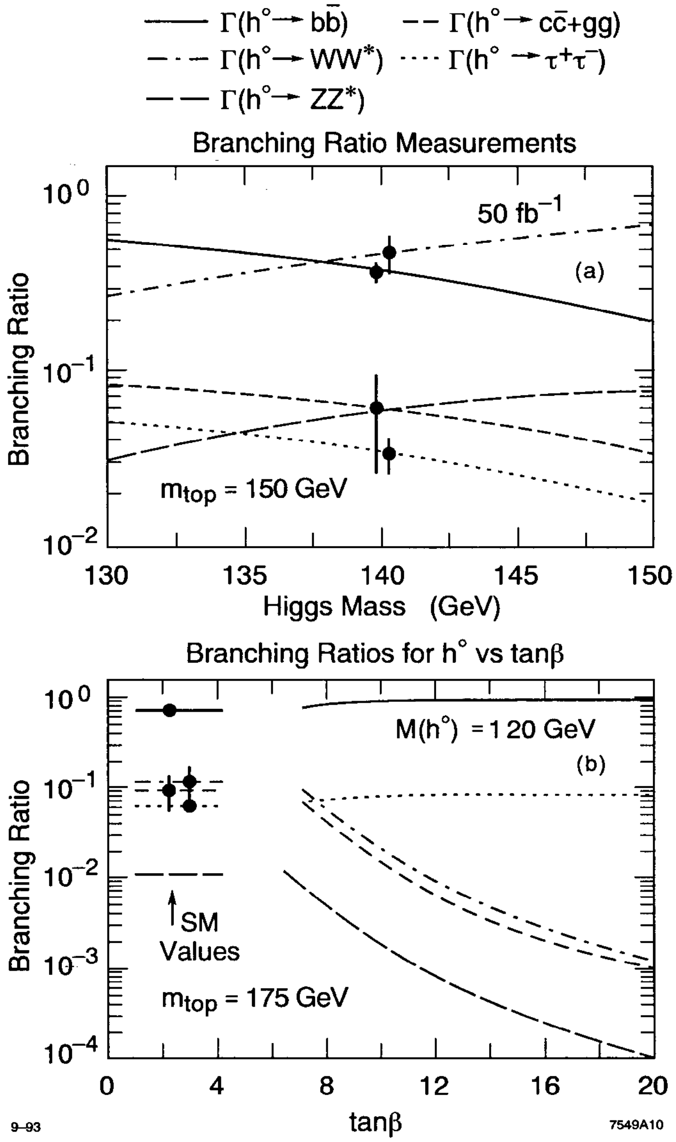

Figure 5. Expectations for Higgs boson branching ratio measurements at a 500 GeV e^+e^- collider, from Ref. [29]. The two figures show simulation results for a Higgs boson of mass 140 GeV and 120 GeV, assuming 50 fb^{-1} of data. The figures (a) and (b) show the theoretical dependence of the branching ratios on m_h and $\tan\beta$.

collider with approximately the original luminosity and 70-80% of the original center-of-mass energy. In such a facility, the Higgs bosons can be produced as resonances in $\gamma\gamma$ scattering, and the partial width $\Gamma(h^0 \to \gamma\gamma)$ can be measured to 10% accuracy [31]. This information and the h^0 total width would complement the measurement of the branching ratio product (7) and allows us to determine the couplings of the h^0 both to photons and to gluons.

For the Higgs sector of supersymmetry, then, the model gives little impetus to go to extremely high energies. An e^+e^- collider running at 500 GeV should produce the lightest

Higgs boson in supersymmetric theories—or in any model where this boson is fundamental at the grand unification scale—and provide a setting for the detailed study of its properties. Such a collider is also, at this same energy, more likely than the LHC to discover the heavy states of the Higgs boson spectrum.

5. Supersymmetry: Superpartners

In addition to providing an interesting Higgs sector, supersymmetric models of electroweak symmetry breaking make the characteristic prediction that the spectrum of elementary particles doubles, with a new scalar for each species of quark and lepton and a new fermion for each gauge boson. If Nature has chosen supersymmetry, the discovery and characterization of these particles will be the major task of the next generation of colliders. In this section, I will compare the expectations for the ability of e^+e^- and pp colliders to investigate these new particles.

To introduce this comparison, I will review some general features of the expected mass spectrum and decay patterns of supersymmetric particles. The phenomenology of supersymmetry is often discussed in a framework in which the model is viewed as part of a grand unified theory with the simplest pattern of supersymmetry breaking. In my discussion, I will use these assumptions to make rough estimates of the mass relations among supersymmetric particles. I will ask whether deviations from these assumptions, which are after all very likely, are observable experimentally. Since supersymmetry is a weak-coupling theory, one can derive detailed predictions from simple assumptions, and it is seductive to consider these predictions as resting on a firm footing. Some of the predictions are, in fact, quite robust with respect to changes in the assumptions; I will point out examples below. Other predictions can change dramatically. From the viewpoint of recommending future colliders, these latter predictions have special interest, because they lead to experimental probes of the mechanism of supersymmetry breaking which comes down from the unification or gravitational scale.

In the simplest type of supersymmetric grand unification, the masses of superpartners are controlled by three mass parameters: m_0, a universal scalar mass, $m_{1/2}$, a universal gaugino mass, and μ, a supersymmetric Higgs boson mass parameter. All three masses are roughly of the size of m_W; a reasonable theory of supersymmetry breaking should explain their near equality. The universality of m_0 and $m_{1/2}$ refers to their values at the scale of grand unification; at lower energies, the masses of different species may differ due to renormalization. For example, in the approximation of one-loop renormalization group equations, the masses of the fermionic partners of the gauge bosons of $SU(3)\times SU(2)\times U(1)$ are expected to obey

$$\frac{m_1}{\alpha_1} = \frac{m_2}{\alpha_2} = \frac{m_3}{\alpha_3} = \frac{m_{1/2}}{\alpha_{\rm GUT}} , \tag{11}$$

where the coupling constants are as in grand unification:

$$\alpha_3 = \alpha_s \ , \qquad \alpha_2 = \frac{\alpha}{\sin^2\theta_w} \ , \qquad \alpha_1 = \frac{5}{3}\frac{\alpha}{\cos^2\theta_w} \ . \tag{12}$$

One consequence of this renormalization is that the (mass)^2 of the Higgs field ϕ_2, which begins at m_0^2 at the grand unification scale, becomes negative at low energy due to loop diagrams involving the top squarks. This is in fact the mechanism of $SU(2)\times U(1)$ breaking in supersymmetric models.

These general ideas lead to a qualitative picture of the superparticle mass spectrum. Most importantly, m_W is a scale of supersymmetry. This scale is generated by the same mass terms which give mass to the superpartners. While it is possible to adjust the parameters of the theory so that m_W is light while the underlying mass parameters are much heavier, this situation is unnatural. In specific models which incorporate this physics, the lighter supersymmetric partners of the W and Z typically have masses below about 200 GeV, with other superpartner masses scaling accordingly [32–36].

The second aspect of this picture is that color singlet superpartners are typically much lighter than colored superpartners. From Eq. (11), we see that the gluino, the partner of the gluon, is by far the heaviest gauge fermion. I will give a precise statement of this relation below. The relation between squark and slepton masses is more model-dependent. At the level of one-loop renormalization group equations, and assuming that both squark and gluino masses are much larger than m_Z, the squark masses at the weak scale obey:

$$m^2(\widetilde{q}) \simeq (0.7m_3)^2 + m_0^2 \ . \tag{13}$$

The first term arises from the squark mass renormalization due to gluino loops. Sleptons acquire a similar, but smaller, mass correction from loop diagrams involving the weak gauge fermions. If the m_0 term dominates Eq. (13), then both squarks and sleptons will be very heavy; in the opposite limit, the slepton masses will be of the same order as the masses of the W superpartners. These renormalizations also lead to mass splittings between the squarks and sleptons associated with right- and left-handed fermions, even for the case of universal scalar masses at the unification scale. These splitting are of order 5% for squarks but should be large for light sleptons. For example, this model predicts the relation

$$m^2(\widetilde{\ell}_L) - m^2(\widetilde{\ell}_R) = (0.6m_{1/2})^2 \ , \tag{14}$$

up to negligible terms proportional to $(1-4\sin^2\theta_w)m_Z^2$.

If we relax the assumption that the scalar masses are universal, many of these detailed results can be upset. Some of the predictions do remain valid in a more general context; in particular, the large positive mass shifts for the gluino and the squarks follow from the renormalization group equations almost irrespective of their initial conditions. On the other hand, the near degeneracy of the squark masses, and the specific pattern of the slepton masses, depends crucially on the model assumptions. If Nature has chosen supersymmetry, we must be able to test these assumptions, and we certainly cannot rely upon them.

The characteristic signatures of supersymmetry at colliders involve the decay of heavier supersymmetric species into the lightest superpartners. Thus, I should begin a discussion of these signatures by reviewing the properties of these lightest states. There are several possibilities for the lightest superparticle: This particle might be a neutral fermion or the scalar partner of the neutrino, and it may or may not be stable with respect to decay to more familiar particles. In this discussion, I will make a particular choice—the one which is least problematical and most thoroughly analyzed—that the lightest superpartner (LSP) is a neutral fermion, and that it is absolutely stable [37].

Under this hypothesis, the LSP is a linear combination of the fermionic partners of the photon, the Z^0, and the two neutral Higgs fields ϕ_1^0 and ϕ_2^0. Supersymmetry requires that these four states mix with one another in a complex pattern. The mass eigenstates are given by diagonalizing the following matrix, written in the $SU(2) \times U(1)$ basis $(\widetilde{B}, \widetilde{A}^3, \widetilde{\phi}_1^0, \widetilde{\phi}_2^0)$:

$$\begin{pmatrix} m_1 & 0 & -m_Z \sin\theta_w \cos\beta & m_Z \sin\theta_w \sin\beta \\ 0 & m_2 & m_Z \cos\theta_w \cos\beta & -m_Z \cos\theta_w \sin\beta \\ -m_Z \sin\theta_w \cos\beta & m_Z \cos\theta_w \cos\beta & 0 & -\mu \\ m_Z \sin\theta_w \sin\beta & -m_Z \cos\theta_w \sin\beta & -\mu & 0 \end{pmatrix} . \tag{15}$$

The parameters m_1, m_2, and μ are determined (or not, as Nature chooses) by the unification relations described above. The entries which are proportional to m_Z are determined by the supersymmetry relations between the couplings of the Higgs fields and those of their fermionic partners. The eigenvectors of this matrix correspond to four massive fermions which are called *neutralinos.* The heavier neutralinos typically decay to the lightest one, the LSP, by emitting weak bosons or quark or lepton pairs.

Similarly, the fermionic partners of the W and charged Higgs bosons mix. This mixing problem is best described by considering partners of W^+ and ϕ_2^+ as the left-handed components of Dirac fermions, while the antiparticles of the partners of W^- and ϕ_1^- are the corresponding right-handed components. This leads to a mass matrix

$$\begin{pmatrix} \widetilde{w}^- & \widetilde{\phi}_1^- \end{pmatrix} \begin{pmatrix} m_2 & \sqrt{2} m_W \sin\beta \\ \sqrt{2} m_W \cos\beta & \mu \end{pmatrix} \begin{pmatrix} \widetilde{w}^+ \\ \widetilde{\phi}_2^+ \end{pmatrix} . \tag{16}$$

The mass eigenstates are called *charginos.*

The lighter of the two charginos, $\widetilde{\chi}_1^+$, has a (mass)^2 less than $(m_2^2 + m_W^2)$. The unification relation between m_2 and m_3, Eq. (11), relates this bound to the mass of the gluino. Taking account of the fact that the physical or 'pole' mass of the gluino is 15-20% higher than the mass m_3 due to QCD corrections [38], we find

$$m^2(\widetilde{\chi}_1^+) < \left(\frac{1}{4} m(\widetilde{g})\right)^2 + m_W^2 . \tag{17}$$

This relation and Eq. (13) quantify the remark made earlier that the color singlet superparticles are typically much lighter than the colored superparticles.

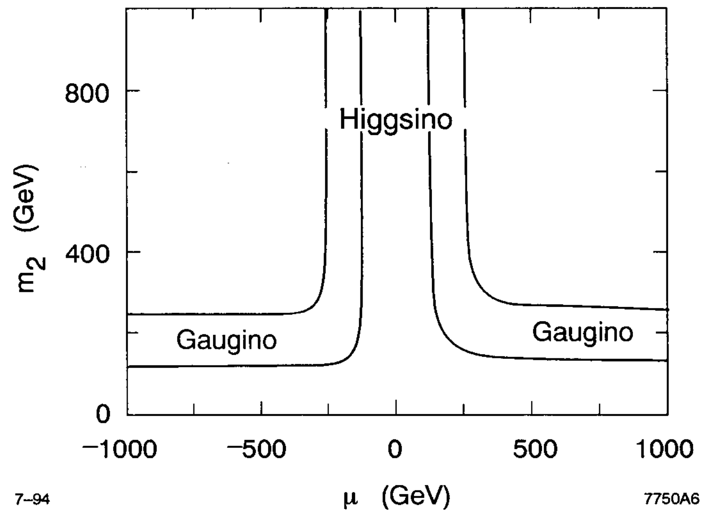

Figure 6. Contours of constant mass of the lighter chargino $\widetilde{\chi}_1^+$ in the (μ, m_2) plane. The two curves correspond to $m(\widetilde{\chi}_1^+) = 125$, 250 GeV, and $\tan\beta = 4$. The labels indicate the regions in which the lightest charginos and neutralinos are mostly gauge boson or mostly Higgs boson superpartners.

The properties of the two chargino eigenstates depend on the relative sizes of all of the parameters in (16). In Fig. 6, I display contours of constant mass for $\widetilde{\chi}_1^+$. In the regions indicated, the lightest chargino and neutralino are mainly gaugino or mainly Higgsino. From one region to another, the decay properties of the chargino and of heavier superparticles change qualitatively. We will see the consequences of this in a moment.

Though the mixing problem of the charginos and neutralinos is complex, there are a few simple features which emerge. Eventually, the heavier charginos and neutralinos, and other heavy superparticles, will decay down to the LSP. This particle then escapes detection, leading to missing transverse momentum and energy. If superpartners have a large production cross section, this signature is robust across the parameter space and is readily observed.

One can search for this missing energy signature quite straightforwardly at high energy pp colliders. Since the gluino is a color octet fermion, it has a large production cross section in gg collisions. The decay products of the gluino include the LSP, which gives rise to events with missing energy. The spectrum of observed missing transverse energy, together with a background estimate made for the SDC detector at the SSC, is shown in Fig. 7. The ATLAS collaboration has estimated that this signature is visible at the LHC up to gluino masses of about 1.6 TeV, assuming a data sample of 100 fb^{-1}, even if squarks are much heavier than gluinos [40]. This goes about a factor 2 beyond the rough theoretical upper limits discussed above.

Once the gluino signature is found, can one establish that this new particle is a superpartner and use its decays to study supersymmetry. It is true that the gluino is free of the mixing problems that we found with the neutralinos, and that it is its own antiparticle. But all other features of the gluino decay are exceedingly complicated. I have already

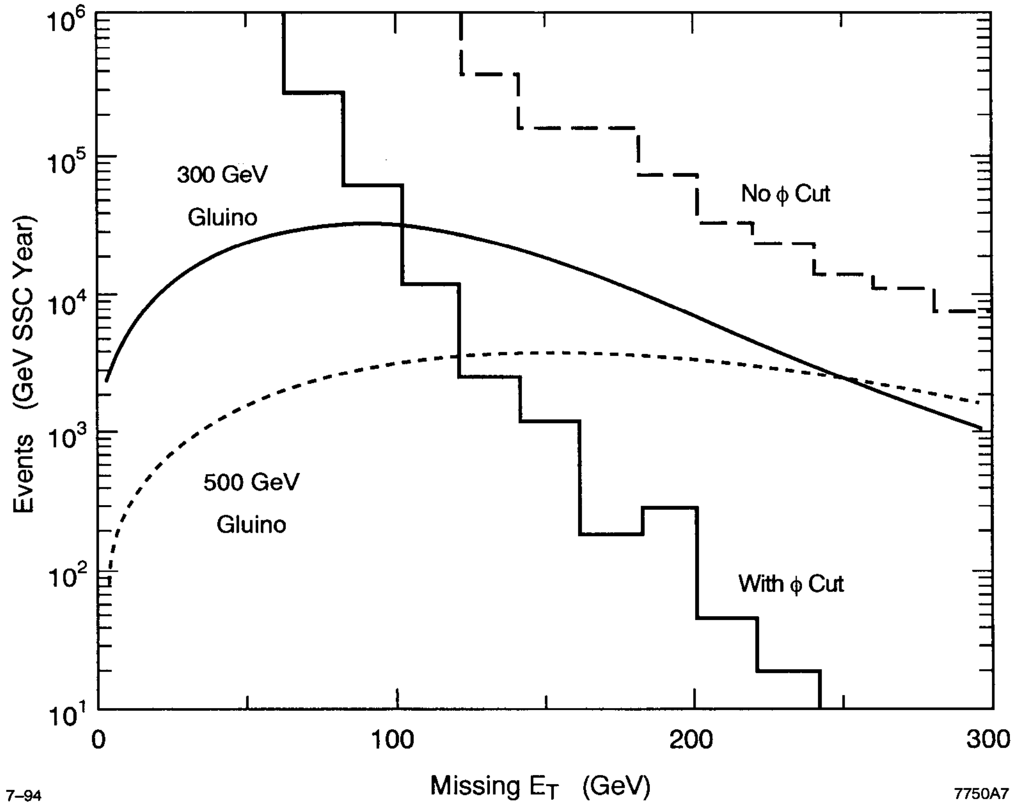

Figure 7. Spectrum of missing transverse energy expected in the SDC detector at the SSC, due to production of gluinos with mass 300 GeV and 500 GeV, from Ref. [39].

pointed out that the gluino is expected to be much heavier than the lightest neutralinos and charginos. Thus, the gluino is expected to decay not only to the lightest particle in this sector but also to the heavier gauge partners, which then decay to the LSP through a complicated decay chain. For example, a decay through the next heaviest superpartners leads to the processes such as

$$\begin{aligned} \widetilde{g} &\rightarrow q\overline{q}\widetilde{\chi}_1^+ \\ &\rightarrow q\overline{q} \quad q\overline{q}\widetilde{\chi}_1^0 \ . \end{aligned} \tag{18}$$

In the these decays and the similar decays to neutralinos, the intermediate steps involve virtual (or real) W, Z, or Higgs bosons, or virtual squarks and sleptons. In simulations of these decay chains, the direct decay to the LSP turns out to be rare, while decays through two or more intermediate superpartners are quite common [41–44]. The model-dependence of the branching fractions of the gluino into various final states is illustrated in Fig. 8.

The complexity of gluino decays has advantages and disadvantages. On the one hand, it leads to a wide variety of gluino signatures, including multilepton and lepton + Z^0 signals in addition to missing E_T. The expected cross sections for these signatures at the LHC, computed at a particular point in the parameter space of the neutralinos and charginos, is shown in Fig. 9. Along with this feature, one cannot avoid the difficulty that the strengths

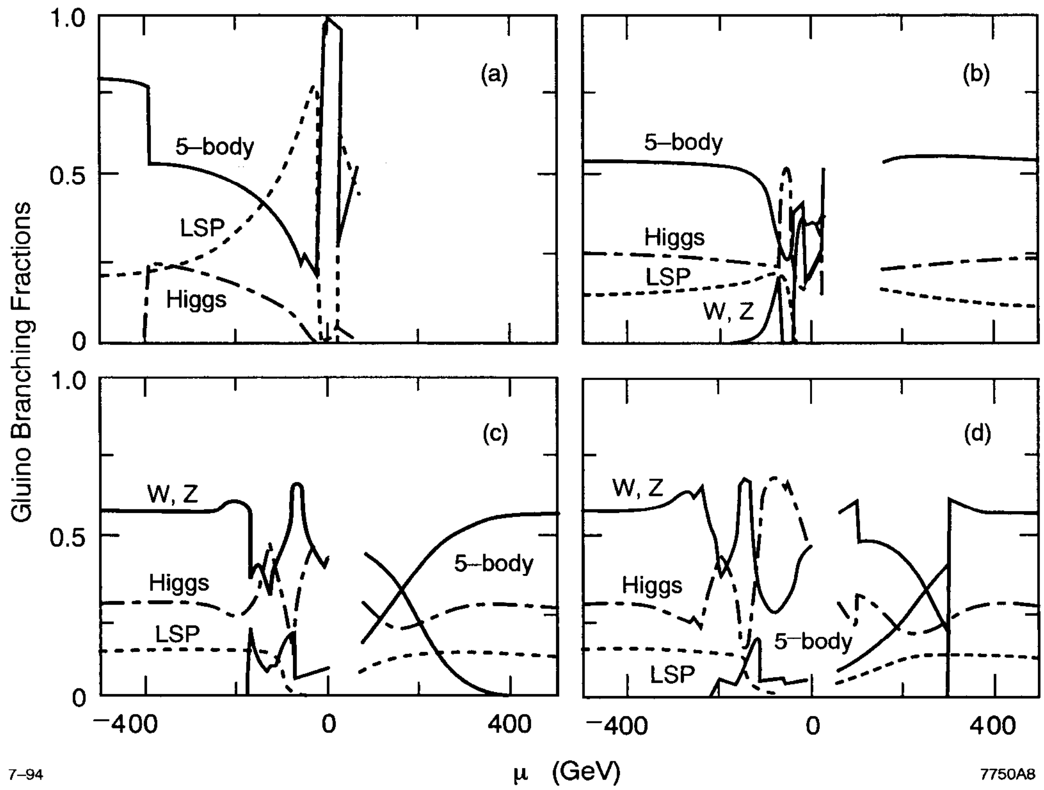

Figure 8. Variation of the gluino branching fractions as a function of μ, for fixed m_2, m_3, from Ref. [42]. The various curves show the branching fractions for direct decay to the LSP, decays to on-shell Higgs bosons, decays to on-shell W and Z bosons, and decays to 5-particle final states. The structure in the center of each diagram is the result of transitions between the gaugino region and the Higgsino region of Fig. 6.

of these signals depend on the properties of the charginos and neutralinos and therefore on the full complexity of the mixing problems (15) and (16). The lower graph in Fig. 9 shows the dependence of the signatures on μ for fixed gluino mass.

In favorable circumstances, some features of these events can provide important pieces of information. Barnett, Gunion, and Haber have pointed out that by combining the momentum vectors of the highest p_T lepton and the two closest jets, one obtains an estimator for the gluino mass. The mass resolution is expected to be about 10%, as shown in Fig. 10. Since the gluino is its own antiparticle, the two hardest leptons are expected to be of like or unlike sign with equal probability, and this property distinguishes supersymmetry from other possible models of new colored fermions. However, neither experiment is unambiguous. Even discounting standard model backgrounds and misidentifications, supersymmetry itself offers many other sources of leptons, for example from squark decays or from the lower stages of $\widetilde{\chi}$ cascades. Under specific circumstances, such as the presence of a light top squark, these new sources not only confuse but actually swamp the more direct lepton signals [46].

Searches for other superparticles have also been considered at hadron colliders, and

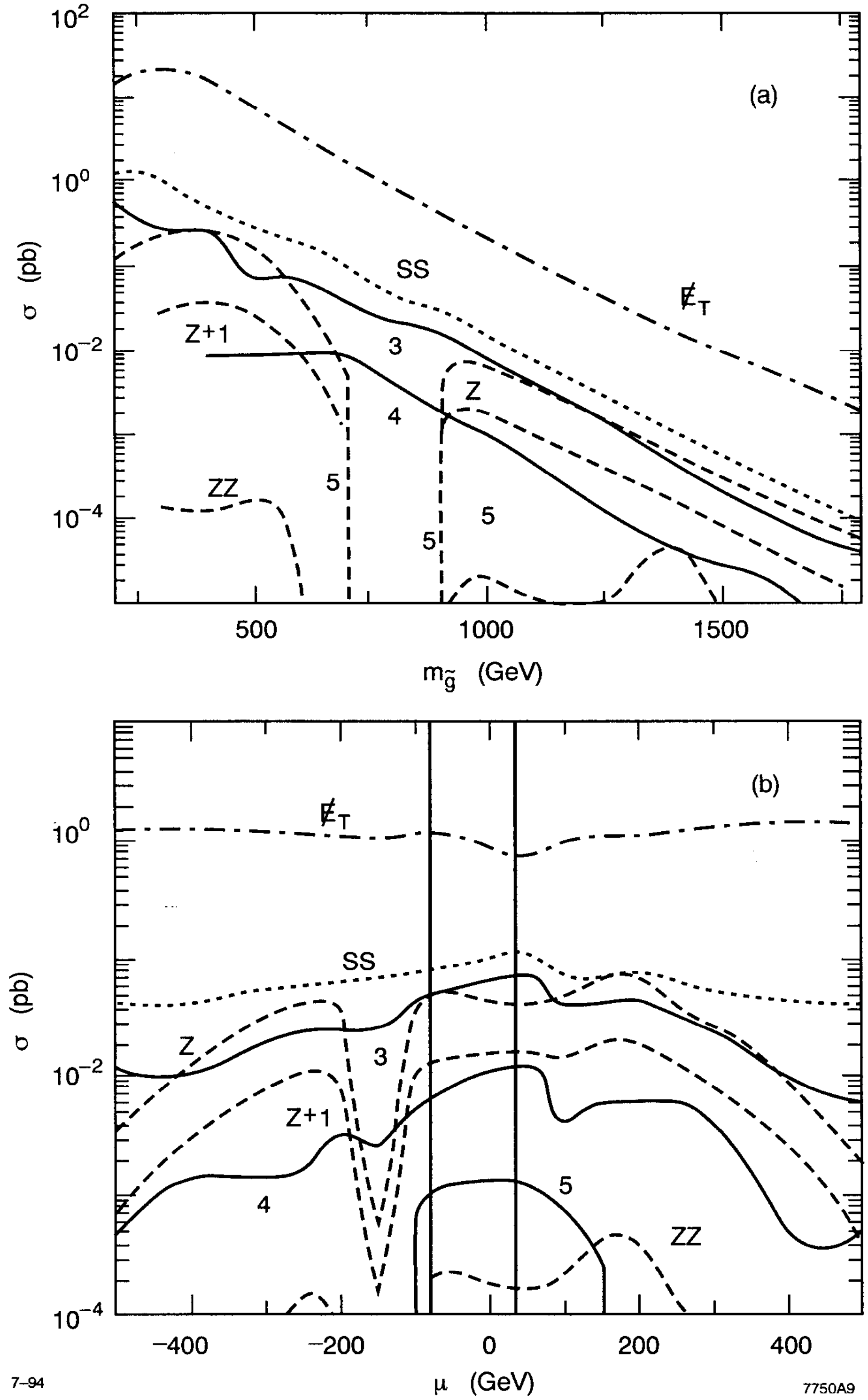

Figure 9. Cross sections expected at the LHC for a variety of signatures of gluino production, from Ref. [44]. The various curves show the cross sections for missing transverse energy, same sign dileptons, and production of the indicated numbers of on-shell Z bosons and isolated leptons, (a) as a function of the gluino mass for μ fixed at -150 GeV, (b) as a function of μ for a gluino mass fixed at 750 GeV.

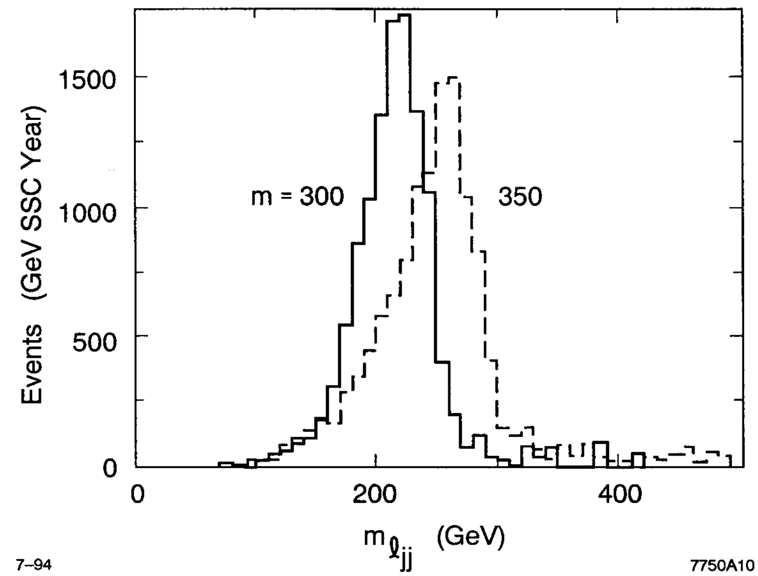

Figure 10. A jet mass combination which estimates the gluino mass, from Ref. [45]. In a simulation for the SSC, events with two isolated like-sign leptons are selected. Then the momentum vector of the highest-p_T lepton is combined with those of the two nearest jets chosen from the four highest-p_T jets. The resulting mass distribution is shown for a gluino of mass 300 GeV and 350 GeV. (The latter histograph is shown divided by two).

these have many of the same opportunities and the same problems that we have seen for the gluino. The production cross section for squarks is similar to that for the gluino, and the technique for mass measurement is similarly indirect. In fact, there is no published method for distinguishing the cases in which squark or gluino production is dominant (though this is certainly a solvable problem). Recently, several groups have studied chargino searches in $q\bar{q}$ annihilation at hadron colliders; this is an interesting production method for relatively light charginos, though it disappears behind the background for chargino masses above about 150 GeV [47,48].

We now turn to supersymmetry signatures at e^+e^- colliders. In principle, any superpartner with nonzero electroweak quantum numbers is produced in e^+e^- annihilation with a substantial cross section. For the purpose of comparison with *pp* colliders, it is important to note that e^+e^- colliders have no difficulty in producing the color singlet superparticles such as charginos. The chargino signal is simple and easily isolated, as has been discussed, for example, by Grivaz [49]. Because these particles are expected to be lighter than their colored counterparts, according to the relation (17), an e^+e^- collider even at 500 GeV in the center of mass is sensitive to a region of supersymmetry parameter space similar to that of a search up to a gluino masses of 1 TeV. This already covers the region expected from the theoretical considerations described above. If one is concerned to push beyond this region, an e^+e^- collider at 1 TeV is actually sensitive to a larger region of supersymmetry parameter space than the LHC.

However, the most important advantages of an e^+e^- collider become apparent at the next stage, when one has found the first signal of supersymmetry. We have seen above that it is very difficult to translate the signatures seen in pp collisions to definite knowledge of the supersymmetry parameters. In e^+e^- collisions, the situation is quite the reverse: One can build up knowledge of the supersymmetry parameters systematically and straightforwardly [50]. There are two important reasons for this special simplicity. First, an e^+e^- collider can directly produce the lightest states of the superparticle spectrum and then characterize the spectrum in stages of increasing mass. Second, an e^+e^- collider offers incisive probes of the superspectrum not available at hadron colliders, especially the handle of electron beam polarization. Tsukamoto, Fujii, Murayama, Yamaguchi, and Okada have clarified this strategy by presenting simulation results on the determination of supersymmetry parameters for a particular choice of the superpartner masses [51]; my discussion will draw strongly on their work.

In contrast to the complex decay pattern we have seen for gluinos, the lightest states in the superspectrum have only a single allowed mode of decay to the LSP. The production mechanism is also much simpler, since the new particles are pair-produced and thus have an energy which is precisely defined, up to minor effects of initial-state radiation. Then the masses of the new state and that of the LSP can be deduced from the endpoints of the energy distribution of observed products. The simplest example is given by the superpartner of the μ_R^-, for which the major decay mode is the 2-body decay $\widetilde{\mu}_R \to \mu + \widetilde{\chi}_1^0$. The muon energy distribution is flat between the endpoints, which can then be read off to an accuracy of 1 GeV. A more typical example is that of the lightest chargino. Figure 11 shows the reconstruction of the dijet energy distribution in the decay $\widetilde{\chi}_1^+ \to q\bar{q}\widetilde{\chi}_1^0$, assuming the detector model of the JLC group. The masses of the $\widetilde{\chi}_1^+$ and the $\widetilde{\chi}_1^0$ are each determined to an accuracy of 2 GeV.

Once we have determined the masses of the lightest charginos and neutralinos, we will also need to determine the mixing angles which relate the underlying basis of superpartners to the mass eigenstates. To some extent, these can be determined from production angular distributions, but the use of electron beams with definite polarization can provide wonderful simplifications. Two reactions which illustrate these simplifications are shown in Fig. 12. In selectron production, shown in Fig. 12(a), the t-channel diagram exists only if the final selectron is the superpartner of the initial electron; thus, choosing e_R^- selects $\tilde{e}_R^-$. Since the e_R^- is a singlet of weak interaction $SU(2)$, the first diagram involves only the $U(1)$ gauge boson B^0, a linear combination of γ and Z^0. Similarly, the t-channel diagram involves only the superpartner $\widetilde{B}^0$ of this boson. By measuring the contribution to the t-channel amplitude from each massive neutralino, one measures the mixing angle between each mass eigenstate and the $\widetilde{B}^0$.

Similarly, in chargino production, Fig. 12(b), the choice of e_R^- removes the t-channel diagram involving sneutrino exchange and allows the measurement of both mixing angles of the chargino. To make this plausible, I will quote the formula for the angular distribution of chargino pair production in the asymptotic limit $\sqrt{s} \gg m_Z, m(\widetilde{\chi}_1^+)$:

$$\frac{d\sigma}{d\cos\theta}(e_R^- e^+ \to \widetilde{\chi}_1^+ \widetilde{\chi}_1^-) \sim \sin^4\phi_+ (1+\cos\theta)^2 + \sin^4\phi_- (1-\cos\theta)^2 \ , \tag{19}$$

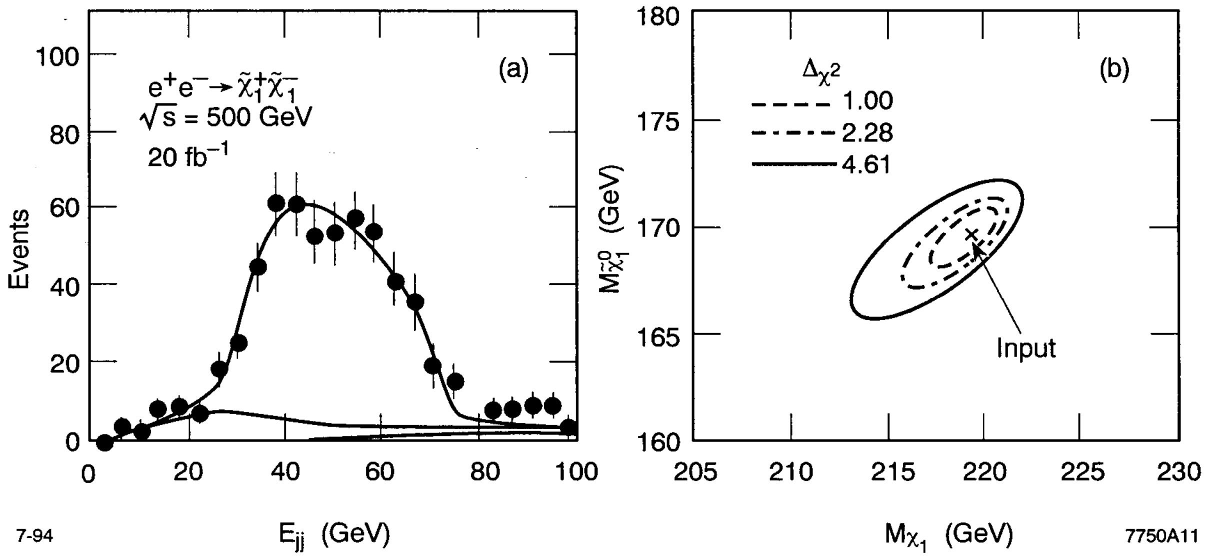

Figure 11. Energy distribution of the 2-jet system produced in the decay $\tilde{\chi}^+ \to \tilde{\chi}^0 q\bar{q}$, as reconstructed in the simulations of Ref. [51]. This work assumes an integrated luminosity of 20 fb^{-1} at an e^+e^- linear collider operating at $\sqrt{s} = 500$ GeV. The right-hand figure shows the χ^2 distribution for the reconstructed masses of $\tilde{\chi}^+$ and $\tilde{\chi}^0$.

where ϕ_+ and ϕ_- are the mixing angles relating the basis of electroweak and mass eigenstates on the right- and left-hand sides of (16). When the second chargino is discovered, in the reaction $e^+e^- \to \tilde{\chi}_1^+\tilde{\chi}_2^-$, the masses of the two charginos M_1, M_2 can be combined with the two mixing angles to reconstruct the off-diagonal elements of the chargino mass matrix. To first order in the mixing angles, this relation reads

$$2m_W^2 = (M_1^2 + M_2^2)(\phi_+^2 + \phi_-^2) - 4M_1M_2\phi_+\phi_- \ . \tag{20}$$

We noted below (15) that m_W appears in the chargino mass matrix by virtue of a supersymmetric relation of couplings. Thus, Eq. (20) provides a simple quantitative test of supersymmetry which can be realized in a large part of parameter space. In other regions, one can alternatively test the supersymmetry relation for the electron-selectron-neutralino and electron-sneutrino-chargino couplings [52].

Another use of the determination of chargino and neutralino mixing angles is to test the unification assumptions discussed at the beginning of this section. Tsukamoto, *et. al.* studied the extent to which one could use the values of the mixing angles obtained from their simulation results to test the relation (11) between m_1 and m_2 and the relation (14) relating the masses of the partners of e_L^- and e_R^-. Their results are shown in Fig. 13. Feng and Finnell have shown that it is also possible to measure mass differences between left- and right-handed quark superpartners at an e^+e^- collider at the level of a few percent, by making use of the polarization-dependence of cross sections [53].

These tests of supersymmetry or supersymmetric unification have no analogue completely within the domain of experiments at pp colliders. However, it is exceedingly inter-

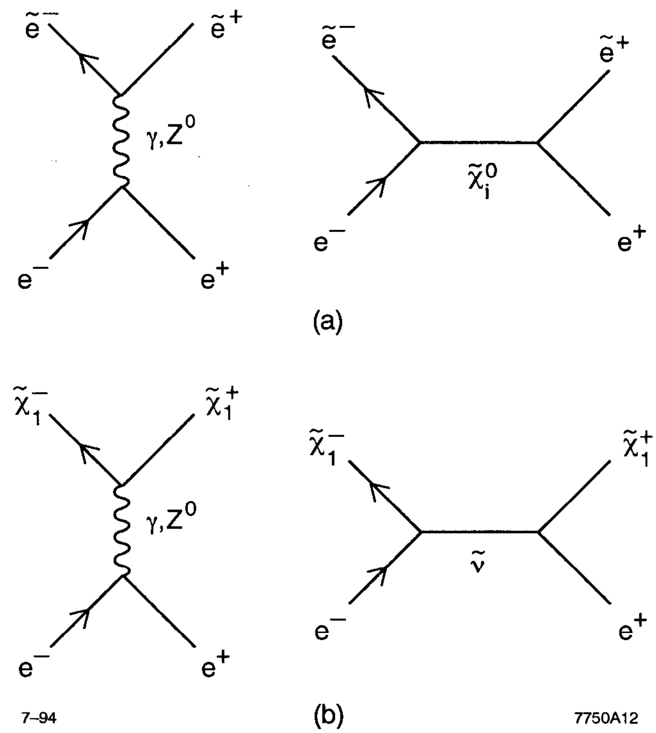

Figure 12. Feynman diagrams contributing to the production of selectron and chargino pairs at e^+e^- colliders. The text describes how these processes illustrate the simplifications obtained by controlling the electron beam polarization.

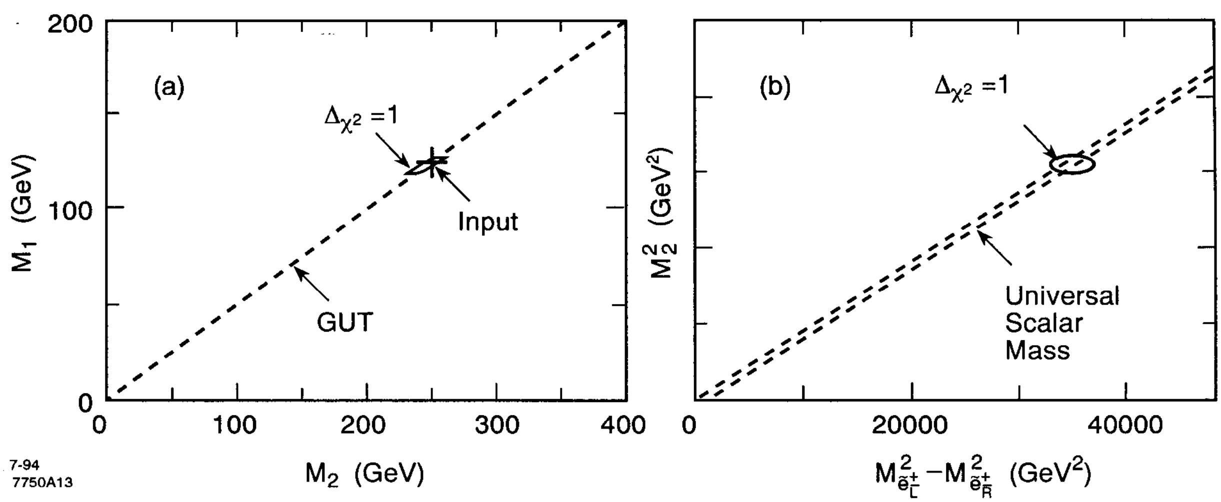

Figure 13. Supersymmetric grand unification tests available at a 500 GeV linear collider in the scenario studied in Ref. [51]: (a) test of the mass relation (11) between the $SU(2)$ and $U(1)$ gauge boson superpartners; (b) test of the mass relation (14) involving the $SU(2)$ gauge boson and the electron superpartners. Both relations require the determination of mixing angles as well as physical particle masses. The two $\chi^2 = 1$ contours include consideration of reconstruction efficiencies and standard model backgrounds.

esting to test the relation between m_2 and m_3, and relations between squark and slepton masses, bringing together information from the two types of facilities. Even more importantly, the measurement of chargino and neutralino masses and mixing angles at e^+e^- colliders will provide an experimental basis for the modeling of squark and gluino cascade decays at hadron colliders. This step may be essential to the process of converting data on hadronic signatures of supersymmetry to quantitative knowledge of the supersymmetry parameters.

6. Technicolor

Now that we have reviewed the experimental prospects for supersymmetry models in some detail, let us turn to the experimental study of technicolor models. Technicolor provides a concrete setting in which strong-coupling physics leads to electroweak symmetry breaking. It is a complete theory, and so it also leads to a variety of observable phenomena which can shed light on the various aspects of the new sector of physics. In this section, I will compare e^+e^- and pp colliders in their ability to observe these various manifestations of technicolor. The most important questions to be answered experimentally are summarized in Table 2.

In the case of supersymmetry, we were able to discuss detailed and quantitative predictions for many phenomena. In the case of technicolor, the predictions we discuss will be more limited. There are two reasons for this: First, the theory includes strong-coupling phenomena, and thus theorists are limited at present to semiquantitative means of calculation. Second, there is no 'technicolor standard model' which is simple, compact, and consistent with all present data. The simplest technicolor models have serious phenomenological problems, and *ad hoc* cures for these problems may remove or alter some of the generic signatures of technicolor.

Since technicolor is based on new strong interactions, the most striking signature of technicolor would be the discovery of the resonances of those interactions. In technicolor models, these resonances are assumed to mirror those of the familiar strong interactions. The states analogous to the pions are eaten by the W and Z to form their longitudinal components. If the flavor symmetry of technicolor is larger than $SU(2) \times SU(2)$, there will be additional observable pseudoscalar mesons, which I will discuss below. But the general, characteristic signal of technicolor is the appearance of an $SU(2)$ triplet of rho resonances. Because the weak bosons contain a techni-pion component, these resonances should appear in WW and WZ scattering in the channel with isospin and spin $I = J = 1$. The mass of the techni-rho is expected to be between 1 and 2 TeV; the resonance is expected to be relatively narrow, with a width of a few hundred GeV.

The physics studies for the SSC included substantial work on the question of experimentally observing the scattering of weak interaction bosons [54–56]. Among the various models considered, the assumption of a narrow techni-rho provides a relatively easy target. In Ref. [57], it is shown that the techni-rho can be reconstructed as a clear peak in the WZ

Table 2: Technicolor

Issues	e^+e^-	pp (LHC)
Techni-rho	visible above 4 TeV as an enhancement of $e^+e^- \to W^+W^-$	visible up to 2 TeV in $(T\rho) \to WZ$
top	ETC effect on t production form factors	ETC $\to t\bar{t} + W$ or Z
Pseudo-Goldstone bosons	PGB's may be colored, but *must* have electroweak charge. visible in $e^+e^- \to P\overline{P}$, up to threshold	visible in $gg \to P\overline{P}$ in $\ell+$ jet modes or in $P \to t\bar{t}$ if P is very light
$S < 0$	spectrum must include light PGB's or light Majorana fermions	

invariant mass spectrum at the LHC (assuming its highest luminosity) if the techni-rho mass is 1.5 TeV; the signal disappears below the background for a techni-rho mass above of 2 TeV.

The techni-rho is also particularly straightforward to observe in e^+e^- annihilation. Just as the conventional rho meson is the dominant effect in the pion form factor, the techni-rho creates a dramatic enhancement in the cross section for $e^+e^- \to W^+W^-$, which is the most important single process in e^+e^- annihilation at high energy [12,58]. The effect of a techni-rho resonance on the differential cross section for W pair production at 90°, for techni-rho masses of 1 and 1.5 TeV, is shown in Fig. 14. Even if the techni-rho resonance is located at much higher energy, its effects are observable if one relies on the ability of e^+e^- colliders to reconstruct W bosons and measure their polarization, and on the fact that the standard model prediction for the W pair production cross section is known to better than 1% accuracy [61]. The sensitivity of e^+e^- colliders to techni-rho resonances of very large mass is shown in Fig. 15.

I should note that this sensitivity to weak boson resonances is special to effects in the $I = J = 1$ channel. There is no analogous reaction which is sensitive to a narrow resonance in the $I = J = 0$ channel. However, there are also no known models which produce such

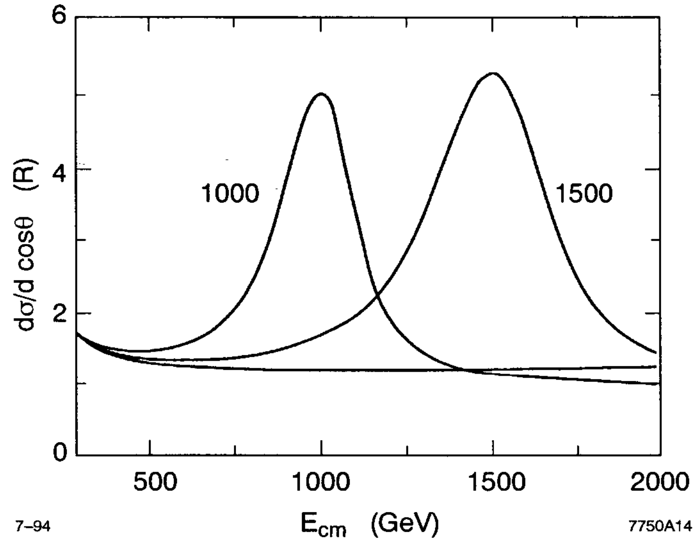

Figure 14. Behavior of the differential cross section for $e^+e^- \to W^+W^-$, $d\sigma/d\cos\theta$ at $\cos\theta = 0$, as a function of $\sqrt{s}$, under in a theory with a techni-ρ resonance at the given mass, from Ref. [59]. The cross section is given in units of R.

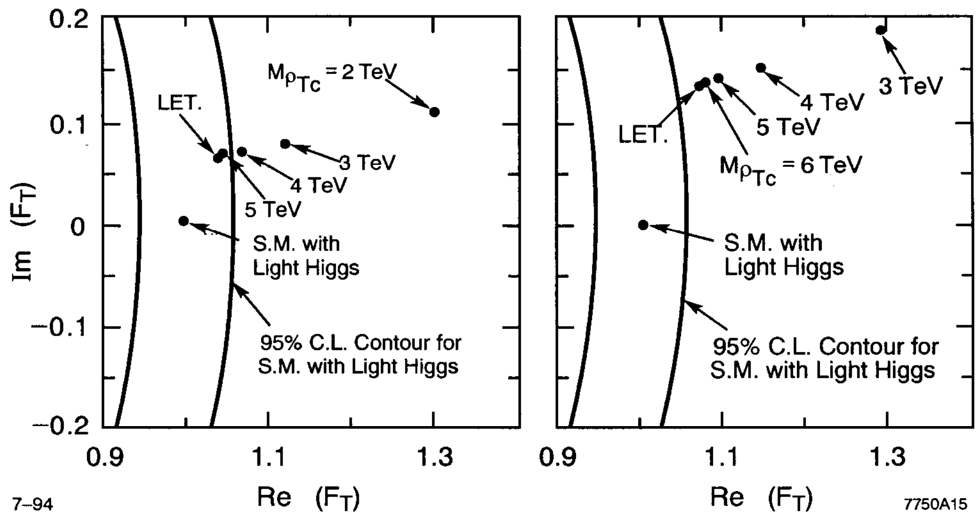

Figure 15. Projected sensitivity of measurements of the differential cross for $e^+e^- \to W^+W^-$ to the presence of a techni-rho resonance, from Ref. [60]. The figure shows the expected constraints on the technicolor analogue of the pion form factor at $Q^2 = s$, and the corresponding predictions for various techni-rho masses. The two figures correspond to a 1 TeV e^+e^- collider with integrated luminosity 200 fb^{-1} and a 1.5 TeV collider with 500 fb^{-1}.

an effect; for example, a minimal Higgs boson at 1.5 TeV has a width of order its mass. In the case of a broad resonance in this channel, the weak boson scattering can be observed at an e^+e^- collider just as at the LHC [62], but the experiment is difficult at both colliders.

If there are more than two flavors of techni-fermions, the technicolor model will produce additional pseudoscalar mesons which are not eaten by the W and Z and which therefore appear as physical particles. These mesons, which unfortunately have the name *pseudo-Goldstone bosons* (pGb's), look much like the CP-odd Higgs bosons of extended Higgs sectors. They are expected to couple most strongly to the heaviest flavors—τ, b, and t. If technifermions carry the color $SU(3)$ of the familiar strong interactions, pGb's may carry color and so may be produced in pp collisions. They are visible as new sources of high transverse momentum top quark or τ lepton pairs, up to masses of about 1 TeV at the LHC [11]. At the same time, pGb's are expected to form singlets and triplets of weak $SU(2)$, and the triplets can be discovered at e^+e^- colliders, in any favored decay mode, up to the pair-production threshold.

To evaluate the relative strength of pp and e^+e^- colliders for this study, it is necessary to have some idea of the masses expected for pGb's. For those pGb's which carry strong interaction quantum numbers, it is easy to compute that standard model radiative corrections give them masses of order 200 GeV [63,64]. However, if only these corrections are included, technicolor models have the dual problems of containing very light charged scalar particles and flavor-changing neutral currents. The natural solution to these problem, due to Holdom [65,66], leads to an additional contribution to the pGb masses which is difficult to calculate and which may be as large as the techni-rho mass. However, Lane and Ramana have recently proposed a variant of this model which contains both colored and charged pGb's below 300 GeV [67].

Once one has invoked new strongly interacting fermions to break electroweak symmetry, it is still necessary to convey this symmetry breaking to obtain masses for the quarks and leptons. In conventional technicolor models, the bridge between the technifermions and the ordinary fermions is made by an additional new set of interactions, called extended technicolor. These new interactions naturally live at scales of order 100 TeV, or even higher in models based on Holdom's ideas. However, the large mass of the top quark requires that at least the particular boson responsible for this mass should have a mass at the 1 TeV scale and also be relatively strongly coupled. Thus, this particular ETC boson should be a target of direct and indirect searches at the next generation of colliders.

The question of direct searches for ETC bosons was studied some time ago by Arnold and Wendt [68]. The lightest ETC boson carries both top quark and technifermion quantum numbers. Thus, it must be pair-produced, and the production process is dominated by s-channel resonances of ETC and anti-ETC bosons bound by technicolor forces. This state then decays to lower mass technicolor bound states as each ETC boson emits a top quark. The end of the chain is a technipion which materializes as a W or Z. The process $gg \to t\bar{t}Z^0$ is expected to be an effective signature for ETC production at the LHC up to masses of about 1.5 TeV. Though a 1.5 TeV e^+e^- collider will not be able to reach the ETC pair resonance at these high energies, one would expect to see the energy-dependent resonance enhancement of $t\bar{t}$ and $t\bar{t}Z^0$ production. At the highest energies, one might see the associated production of t quarks with $\overline{\mathrm{ETC}}$-technifermion bound states.

More generally, the ETC renormalization of the top quark form factors should produce effects of order $(m_t/m_{\mathrm{ETC}})^2$ in the energy dependence of t quark pair production and may produce an effect of order (m_t/m_{ETC}) in the normalization of the $t\bar{t}Z^0$ form factor [69]. If these effects are of the expected size, they will require for their detection the control over the shape and absolute normalization of form factors at the few percent level available only at an e^+e^- collider. (At this moment, there is much speculation about larger effects, based on anomalies in the distribution of the first top quark events reported by CDF [70].) In any event, e^+e^- colliders offer many handles for the separation and measurement of the top quark production and decay form factors, in particular, a large polarization asymmetry which results from γ–Z interference [59].

To conclude this section, I should point out that the version of technicolor phenomenology that I have presented here is rather conservative, to the extent that it does not take into account all known difficulties of the technicolor scheme. A techni-rho of the size discussed above creates electroweak radiative corrections which are now excluded by the precision Z^0 data at the 3 σ level. This problem can be cured by including exotic pGb's or Majorana fermions with mass about 100 GeV [71,72]; these would be naturally found at e^+e^- colliders. The version of ETC discussed by Arnold and Wendt has difficulty in producing a top quark mass above 100 GeV; the cure for this problem may dilute their direct ETC signal, but it may also provide new corrections to the top quark form factors. It is not obvious whether the version of technicolor chosen by Nature will include new high-energy signatures or new corrections to the properties of the W and t which couple strongly to this sector. We should be prepared to look for both of these effects.

7. Conclusions

In this lecture, I have tried to make a reasoned comparison of the capabilities of the next generation of e^+e^- and pp colliders. I have taken as my starting point the idea that the goal of the next colliders to discover the mechanism of electroweak symmetry breaking. I have taken seriously that idea that electroweak symmetry breaking has an explanation in physics, and that this explanation requires a new sector of forces and interactions. To evaluate the relative power of electron and hadron experiments, we must study models of symmetry breaking in their entirety, looking at the variety of phenomena that each model makes available and comparing the very different signatures the colliders access at comparable values of the underlying parameters.

I have presented a broad survey of this sort for supersymmetry and technicolor models of electroweak symmetry breaking. I do not insist that one of these models is chosen by Nature as the solution to the problem of electroweak symmetry breaking. Rather, I am attracted to these models because they have been thoroughly analyzed in the literature, and that analysis can form the groundwork for the broad-based comparison that I have argued is required. Since supersymmetry models are well characterized quantitatively, we were able to make detailed comparisons of processes available to e^+e^- and pp experiments. In the case of technicolor models, the comparisons we made were more rough and indicative. However, the conclusions derived from these two very different models are surprisingly similar.

Most strikingly, this comparison highlights the complementarity of e^+e^- and pp experimentation. For almost every phenomenon available to the LHC, we identified a signature of new physics at an e^+e^- collider which addresses the same issue from a different viewpoint. At times, these signatures were quite similar, as in the example of the resonant effect of the technirho on WZ and WW production, but at other times they involved completely different experiments, for example, the comparison of chargino masses in e^+e^- to the gluino mass observed in pp collisions.

In both models, the values of e^+e^- center of mass energy at which these complementary signatures become available was much lower that the value inferred from the criterion of 'discovery reach'. In fact, in both models, e^+e^- experiments at 500 GeV in the center of mass already would have a significant impact. In supersymmetric models, an e^+e^- collider at this energy would already cover the complete allowed mass region for the lightest Higgs boson, allowing the detailed characterization of this state, including the measurement of decay branching ratios. It would also cover the expected region for pair-production of the lightest chargino. In technicolor models, a 500 GeV e^+e^- collider would allow precision measurement of the top quark form factors, giving a window into ETC physics as likely as any we discussed. Though technicolor models seemed to put more of a premium on experiments at high energy, we saw that, at about 1 TeV in the supersymmetry case and at about 1.5 TeV in the technicolor case, an e^+e^- collider would surpass the LHC in providing experimental information on the new sector of interactions.

In addition, we saw several examples in which information from e^+e^- colliders is needed to fully interpret the experimental results obtained from pp colliders. We saw this connection most clearly in the case of supersymmetry, where the theory makes detailed predictions for the properties of the Higgs boson and the gluino which depend on a complex of model parameters, and where e^+e^- colliders provide a systematic program for determining those parameters. It is quite likely that, if a quantitative technicolor model of the top quark mass could be found, experiments on large transverse momentum top production in pp colliders would have the same relation to e^+e^- precision measurements of the top quark properties at threshold.

From all of these considerations, I conclude that an e^+e^- linear collider, scaleable in energy but beginning at 500 GeV in the center of mass, will play an essential role in the experimental solution of the problem of electroweak symmetry breaking. It follows that we should plan to make such a facility available *simultaneously* with the LHC.

The creation of two new accelerator facilities, each with a cost in the billions of dollars, is not a simple task. For most of the lifetime of our field, we have justified the construction of new facilities through international or inter-regional competition. Almost twenty years ago, Professor Yoshio Yamaguchi, the long-time director of this series of workshops, introduced a different vision of high-energy physics, based on global cooperation in international facilities. When I first visited Japan in 1985, Professor Yamaguchi's vision seemed hopelessly idealistic, at a time when the SSC and the LHC were being pursued as competitive regional projects which would exhaust our global resources. Today, it is an idea whose time has finally come. I hope that Professor Yamaguchi's vision can be combined with a clear appreciation of the physics issues of the coming generation of colliders to provide the tools we will need to understand the next level of the fundamental interactions.

Acknowledgements:

I am grateful to Professor Sakue Yamada for the invitation to present this lecture, and to Tim Barklow, David Burke, Jonathan Feng, Howard Haber, Gordon Kane, Hitoshi Murayama, Thomas Rizzo, Xerxes Tata, and many other colleagues at SLAC and elsewhere for discussion of the issues raised here.

REFERENCES

1. LHC Study Group, *Design Study of the Large Hadron Collider.* (CERN, 1991).
2. G. Loew, in *Proceedings of the ECFA Workshop on e^+e^- Linear Colliders (LC92),* R. Settles, ed. (MPI Munich, 1993).
3. B. Wiik, in *Physics and Experiments with Linear e^+e^- Colliders,* vol. I, F. A. Harris, S. L. Olsen, S. Pakvasa, and X. Tata, eds. (World Scientific, Singapore, 1993).
4. L. Susskind, *Phys. Rev.* **D20,** 2619 (1979).
5. H. P. Nilles, *Phys. Repts.* **110,** 1 (1984).
6. H. E. Haber and G. L. Kane, *Phys. Repts.* **117,** 75 (1985).
7. P. Langacker and M.-X. Luo, *Phys. Rev.* **D44,** 817 (1991).
8. R. Kaul, *Rev. Mod. Phys.* **55,** 449 (1983).
9. K. Lane, in *Proceedings of the Theoretical Advanced Study Institute (TASI 93), S. Raby, ed. (World Scientific, Singapore, 1994).*
10. *G. L. Kane and M. L. Perl, in Elementary Particle Physics and Future Facilities* (Snowmass 1982), R. Donaldson, R. Gustafson, and F. Paige, eds. (Fermilab, 1982).
11. E. Eichten, I. Hinchliffe, K. Lane, and C. Quigg, *Rev. Mod. Phys.* **56,** 579 (1984).
12. M. E. Peskin, in *Physics in Collision 4,* A. Seiden, ed. (Éditions Frontières, Gif, 1984).
13. U. Amaldi, in *Proceedings of the Workshop on Future Accelerators,* vol. I, J. H. Mulvey, ed. (CERN, 1987).
14. A. J. Weinstein, in *Proceedings of the 1989 International Symposium on Lepton and Photon Interactions at High Energies,* M. Riordan, ed. (World Scientific, Singapore, 1990).
15. H. Haber, in *Perspectives on Higgs Physics,* G. L. Kane, ed. (World Scientific, Singapore, 1992).
16. N. Cabbibo, L. Maiani, G. Parisi, and R. Petronzio, *Nucl. Phys.* **B158,** 295 (1979).
17. G. L. Kane, C. Kolda, and J. D. Wells, *Phys. Rev. Lett.* **70,** 2686 (1993).

18. J. F. Gunion, H. E. Haber, G. Kane, and S. Dawson, *The Higgs Hunter's Guide.* (Addison Wesley, Redwood City, 1990).

19. Z. Kunszt and F. Zwirner, *Nucl. Phys.* **B385,** 3 (1992).

20. J. F. Gunion and L. H. Orr, *Phys. Rev.* **D46,** 2052 (1992).

21. H. Baer, M. Bisset, C. Kao, and X. Tata, *Phys. Rev.* **D46,** 1067 (1992).

22. V. Barger, K. Cheung, R. J. N. Phillips, and A. L. Stange, *Phys. Rev.* **D46,** 4914 (1992).

23. M. Felcini, in *Proceedings of the Large Hadron Collider Workshop,* vol. II, G. Jarlskog and D. Rein, eds. (CERN, 1990).

24. J. Dai, J. F. Gunion, and R. Vega, Phys. Lett. **B315,** 355 (1993), UCD-94-7 (1994).

25. S. Mrenna and G. L. Kane, CALT-68-1938 (1994).

26. J. F. Gunion and H. E. Haber, *Phys. Rev.* **D48,** 5109 (1993).

27. K. Kawagoe and S. Orito, in *Proceedings of the Third Workshop on the Japan Linear Collider,* A. Miyamoto, ed. (KEK, 1992).

28. P. Janot, in *Physics and Experiments with Linear e^+e^- Colliders,* vol. I, F. A. Harris, S. L. Olsen, S. Pakvasa, and X. Tata, eds. (World Scientific, Singapore, 1993).

29. M. D. Hildreth, T. L. Barklow, and D. L. Burke, *Phys. Rev.* **D49,** 3441 (1994).

30. V. Telnov, in *Physics and Experiments with Linear Colliders,* Vol. II, R. Orava, P. Eerola, and M. Nordberg, eds. (World Scientific, Singapore, 1992).

31. D. L. Borden, D. A. Bauer, and D. O. Caldwell, *Phys. Rev.* **D48,** 4018 (1993).

32. R. Barbieri, in *Z Physics at LEP 1,* G. Altarelli, R. Kleiss, and C. Verzegnassi, eds, vol. 2. (CERN, Geneva, 1989).

33. G. G. Ross and R. G. Roberts, *Nucl. Phys.* **B377,** 571 (1992).

34. R. Arnowitt and P. Nath, *Phys. Rev. Lett.* **69,** 725 (1992).

35. S. Kelley, J. L. Lopez, D. V. Nanopoulos, H. Pois, and K. Yuan, *Nucl. Phys.* **B398,** 3 (1993).

36. G. L. Kane, C. Kolda, L. Roszkowski, and J. D. Wells, UM-TH-93-24 (1993).

37. For discussion of other options, see Ref. [6] and S. Dimopoulos and L. Hall, *Phys. Lett.* **207B,** 210 (1988).

38. S. P. Martin and M. T. Vaughn, *Phys. Lett.* **B318,** 331 (1993); D. Pierce and A. Papadopoulos, JHU-TIPAC-940001 (1994).

39. Solenoidal Detector Collaboration (SDC), *Technical Design Report.* (SSC Laboratory, 1992).

40. G. Polesello, in *International Workshop on Supersymmetry and the Unification of the Fundamental Interactions,* P. Nath, ed. (World Scientific, Singapore, 1993).

41. H. Baer, V. Barger, D. Karatas, and X. Tata, *Phys. Rev.* **D36,** 96 (1987).

42. R. M. Barnett, J. F. Gunion, and H. E. Haber, *Phys. Rev.* **D37,** 1892 (1988).

43. H. Baer, X. Tata, and J. Woodside, *Phys. Rev.* **D42,** 1568 (1990).

44. H. Baer, X. Tata, and J. Woodside, *Phys. Rev.* **D45,** 142 (1992).

45. R. M. Barnett, J. F. Gunion, and H. E. Haber, in *Research Directions for the Decade (Snowmass, 1990),* E. L. Berger, ed. (World Scientific, Singapore, 1992).

46. H. Baer, M. Drees, C. Kao, M. Nojiri, and X. Tata, FSU-HEP-940311 (1994).

47. J. L. Lopez, D. V. Nanopoulos, X. Wang, and A. Zichichi, *Phys. Rev.* **D48,** 2062 (1993).

48. H. Baer, C. Kao, and X. Tata, *Phys. Rev.* **D48,** 5175 (1993); H. Baer, C. Chen, F. Paige, and X. Tata, FSU-HEP-940310 (1994).

49. J.-F. Grivaz, in *Physics and Experiments with Linear Colliders,* Vol. I, R. Orava, P. Eerola, and M. Nordberg, eds. (World Scientific, Singapore, 1992).

50. S. Orito, in *Physics and Experiments with Linear e^+e^- Colliders,* vol. I, F. A. Harris, S. L. Olsen, S. Pakvasa, and X. Tata, eds. (World Scientific, Singapore, 1993).

51. T. Tsukamoto, K. Fujii, H. Murayama, M. Yamaguchi, and Y. Okada, KEK-PREPRINT-93-146 (1993).

52. J. Feng, H. Murayama, M. E. Peskin, and X. Tata, in preparation.

53. J. L. Feng and D. E. Finnell, *Phys. Rev.* **D49,** 2369 (1994).

54. M. S. Chanowitz and M. K. Gaillard, *Nucl. Phys.* **B21,** 379 (1985).

55. M. S. Chanowitz and W. Kilgore, *Phys. Lett.* **B322,** 147 (1994).

56. J. Bagger, *et. al.*, *Phys. Rev.* **D49,** 1246 (1994).

57. I. Josa, F. Pauss, and T. Rodrigo, in *Proceedings of the Large Hadron Collider Workshop,* vol. II, G. Jarlskog and D. Rein, eds. (CERN, 1990).

58. F. Iddir, A. Le Yaouanc, L. Oliver, O. Pene, and J. C. Raynal, *Phys. Rev.* **D41,** 22 (1990).

59. M. E. Peskin, in *Physics and Experiments with Linear Colliders,* Vol. I, R. Orava, P. Eerola, and M. Nordberg, eds. (World Scientific, Singapore, 1992).

60. T. L. Barklow, in *Physics and Experiments with Linear Colliders,* Vol. I, R. Orava, P. Eerola, and M. Nordberg, eds. (World Scientific, Singapore, 1992).

61. W. Beenakker, A. Denner, S. Dittmar, R. Mertig, and T. Sack, *Nucl. Phys.* **B410,** 245 (1993); W. Beenakker and A. Denner, DESY-94-051 (1994).

62. Y. Kurihara and R. Najima, *Phys. Lett.* **B301,** 292 (1993).

63. M. E. Peskin, *Nucl. Phys.* **B175,** 197 (1980).

64. J. P. Preskill, *Nucl. Phys.* **B177,** 21 (1981).

65. B. Holdom, *Phys. Rev.* **D24,** 1441 (1981).

66. T. Appelquist, D. Karabali, and L. C. R. Wijewardhana, *Phys. Rev. Lett.* **57,** 957 (1986).

67. K. Lane and M. V. Ramana, *Phys. Rev.* **D44,** 2678 (1991).

68. P. Arnold and C. Wendt, *Phys. Rev.* **D33,** 1873 (1986).

69. R. S. Chivukula, S. Selipsky, and E. H. Simmons, *Phys. Rev. Lett.* **69,** 575 (1992); R. S. Chivukula, E. H. Simmons, and J. Terning, *Phys. Lett.* **B311,** 383 (1994).

70. F. Abe, *et. al.*(CDF Collaboration), *Phys. Rev. Lett.* **73,** 225 (1994).

71. M. J. Dugan and L. Randall, *Phys. Lett.* **B264,** 154 (1991).

72. E. Gates and J. Terning, *Phys. Rev. Lett.* **67,** 1840 (1991).